

## Supplementary Information

### ***In vitro* digestion of high-lipid emulsions: towards a critical interpretation of lipolysis**

Paula K. Okuro<sup>1,2</sup> Michèle Viau<sup>1</sup>, Sébastien Marze<sup>1</sup>, Sophie Laurent<sup>1</sup>, Rosiane L. Cunha<sup>2</sup>, Claire Berton-Carabin<sup>1,3\*</sup>, Anne Meynier<sup>1\*</sup>

<sup>1</sup>INRAE, UR BIA, F-44316, Nantes, France, <sup>2</sup>Department of Food Technology and Engineering, School of Food Engineering, University of Campinas, 13083-862, Campinas, Brazil, <sup>3</sup>Laboratory of Food Process Engineering, Wageningen University & Research, 6700 AA, Wageningen, The Netherlands

\*corresponding authors: anne.meynier@inrae.fr, claire.berton-carabin@inrae.fr

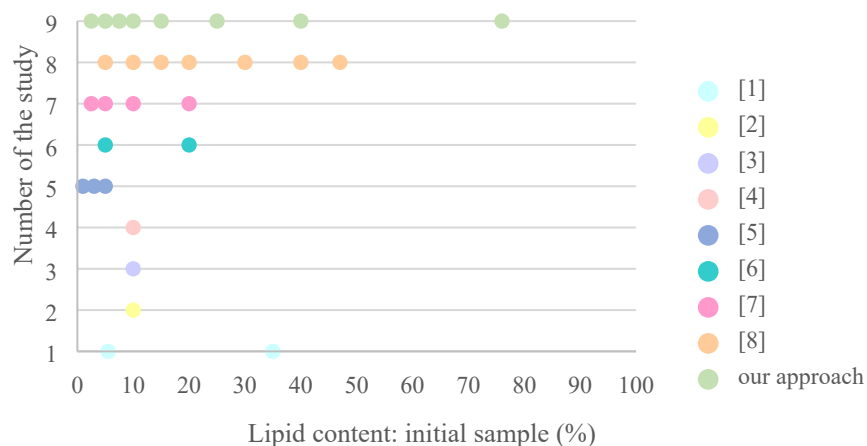
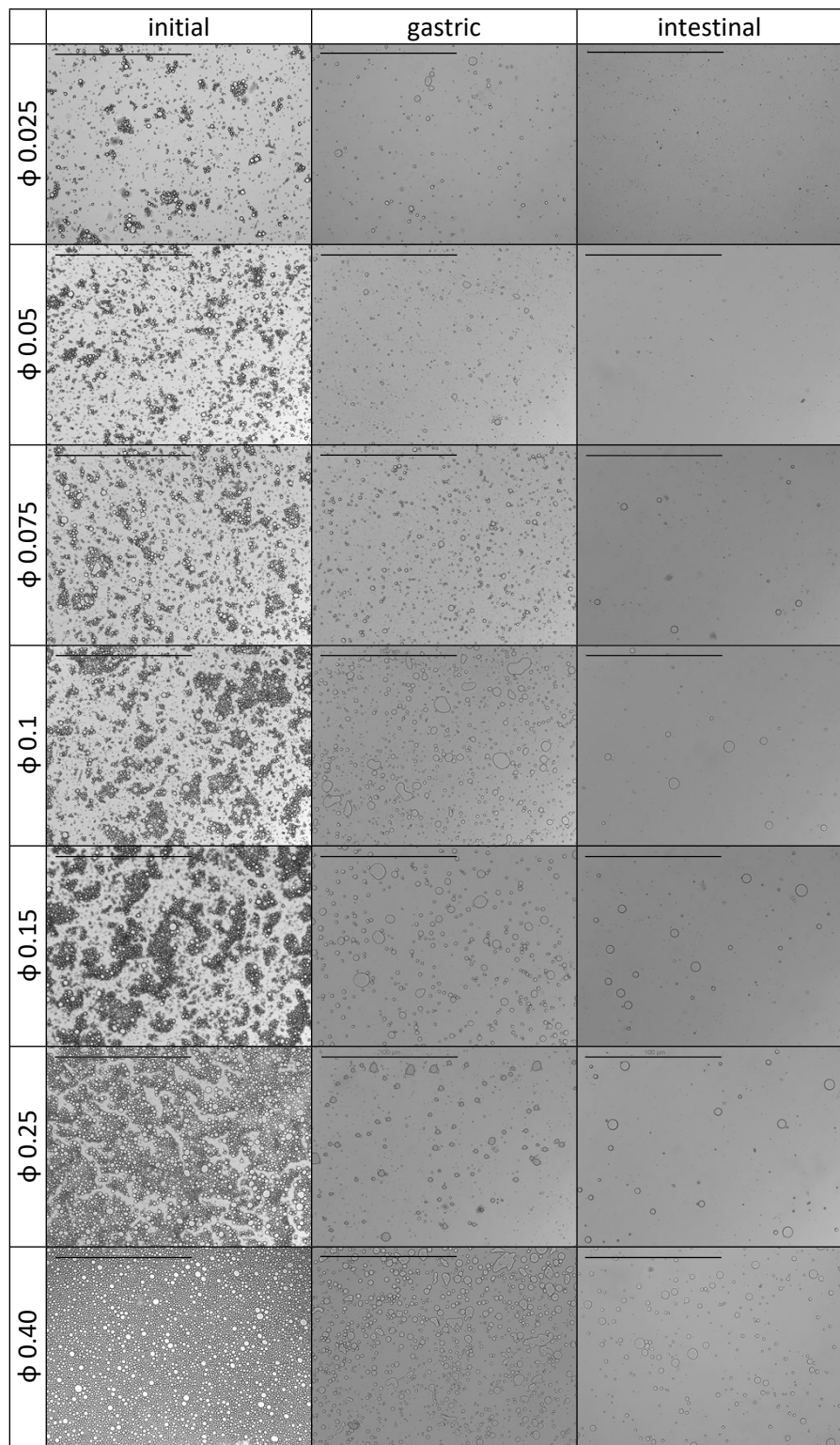


Fig. S1. Overview of the available literature on the effect of the lipid content on *in vitro* digestion in oil-in-water emulsions. [1] J. Calvo-Lerma, V. Fornés-Ferrer, A. Heredia and A. Andrés, Food Res. Int., 2019, 125, 108511; [2] K. Ahmed, Y. Li, D. J. McClements and H. Xiao, Food Chem., 2012, 132, 799–807; [3] Y. Li, M. Hu and D. J. McClements, Food Chem., 2011, 126, 498–505; [4] Y. Li and D. J. McClements, J. Agric. Food Chem., 2010, 58, 8085–8092; [5] K. Yao, D. J. McClements, C. Yan, J. Xiao, H. Liu, Z. Chen, X. Hou, Y. Cao, H. Xiao and X. Liu, Food Res. Int., 2021, 141, 110162; [6] S. H. E. Verkempinck, J. M. Guevara-Zambrano, M. R. Infantes-Garcia, M. C. Naranjo, R. Soliva-Fortuny, P. Elez-Martínez and T. Grauwet, Food Biosci., 2022, 46, 101595; [7] Y. Tan, Z. Zhang, H. Zhou, H. Xiao and D. J. McClements, Food Funct., 2020, 11, 7126–7137; [8] S. Martínez, M. Espert, A. Salvador and T. Sanz, Food Hydrocoll., 2022, 131, 107793; [9] Our study.



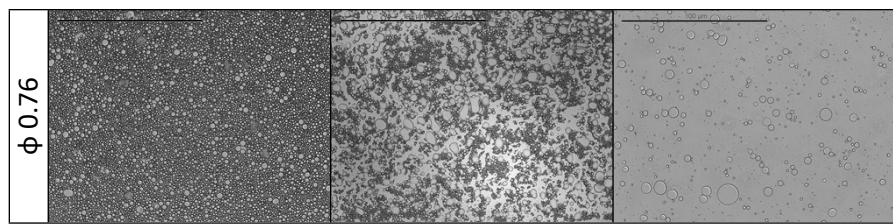


Fig. S2. Optical microscopy of emulsion samples (i) before starting digestion (“meal”) and after (ii) gastric and (iii) intestinal *in vitro* digestion phases. The scale bar is 100  $\mu\text{m}$ .

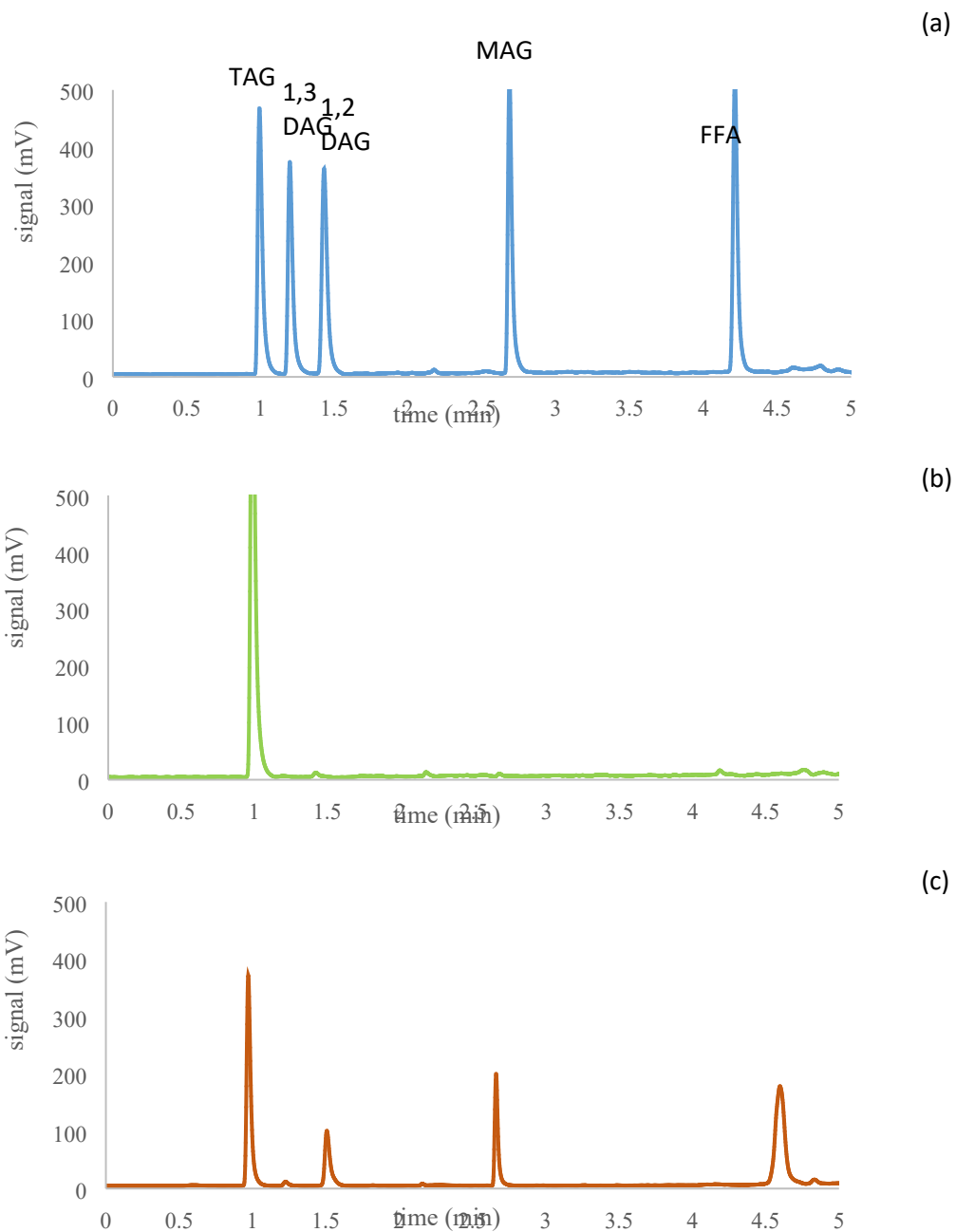
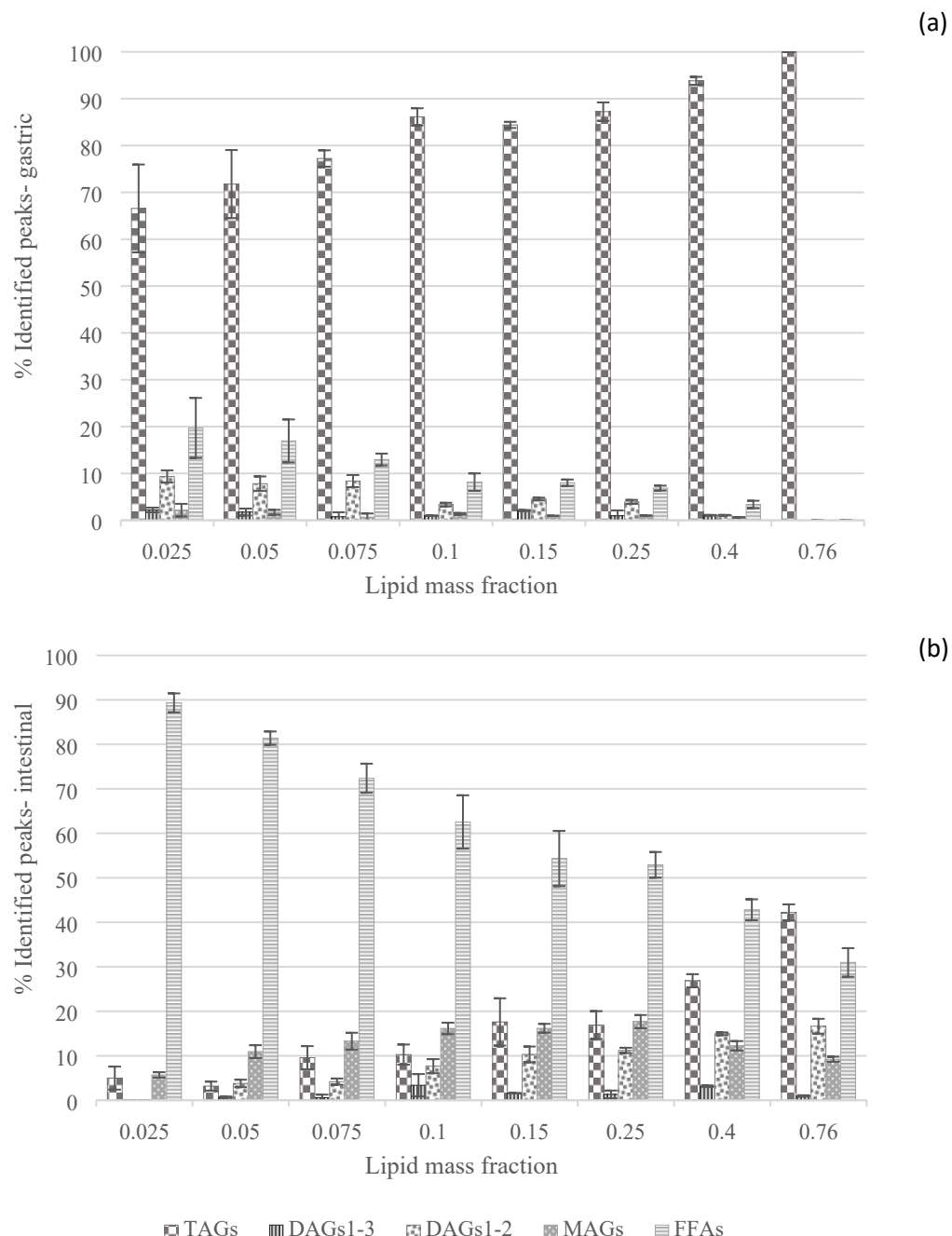


Fig. S3. Representative normal phase chromatograms of standard compounds (4  $\mu$ g each compound injected) (a); of the lipid extract at the end of the gastric step  $\phi=0.25$  (oral + gastric steps) (b) and; of the lipid extract at the end of the intestinal phase (oral + gastric + intestinal steps)  $\phi=0.25$  (c).



**Fig. S4.** Lipid species (TAGs, DAGs<sub>1-3</sub>, DAGs<sub>1-2</sub>, MAGs and FFAs) present in the digestive medium (% of identified peaks) assessed by HPLC analysis at the endpoint of gastric (a) and intestinal (b) phases, respectively, as a function of the oil mass fraction in the initial emulsion (n=4).

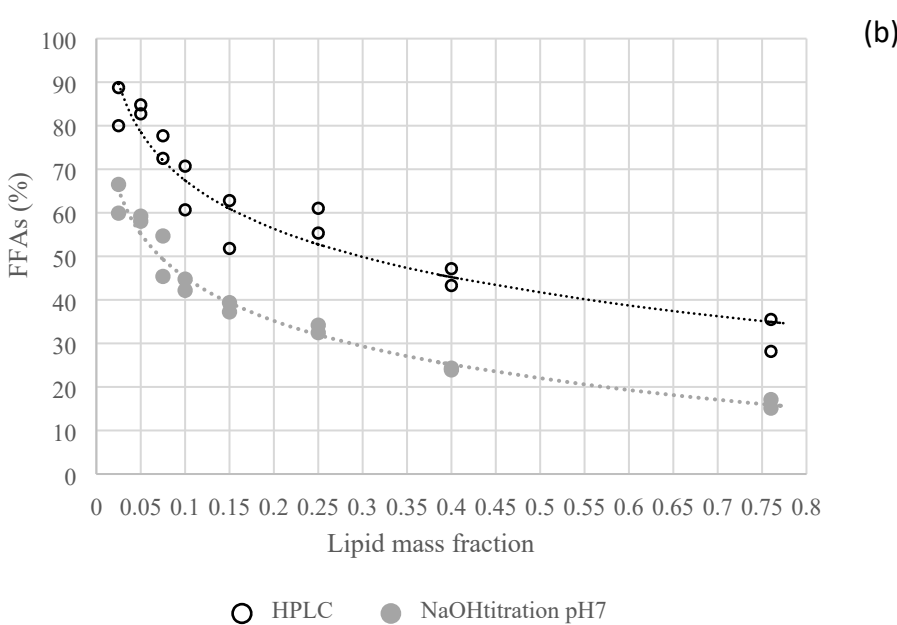
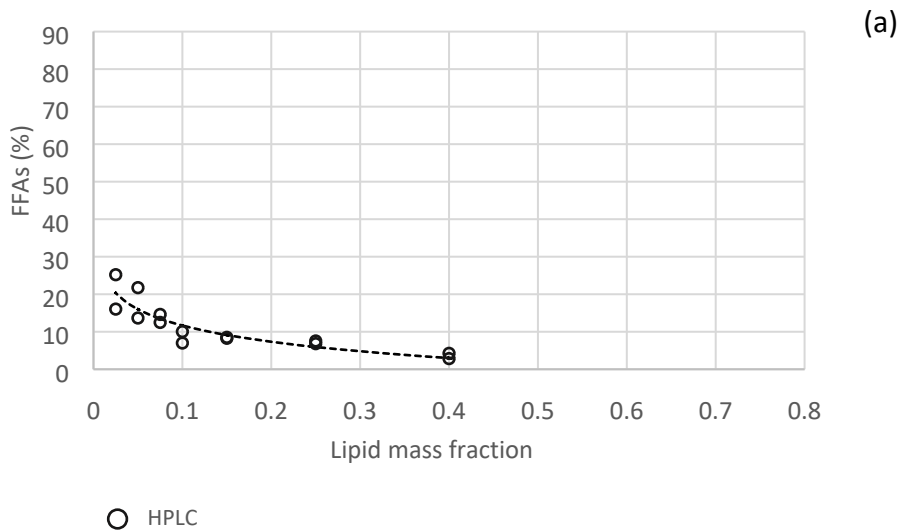


Fig. S5. Lipolysis extent determined at the endpoint of gastric (a) and intestinal (b) phases, either via identification and quantification of the lipid classes by HPLC, or via NaOH titration.

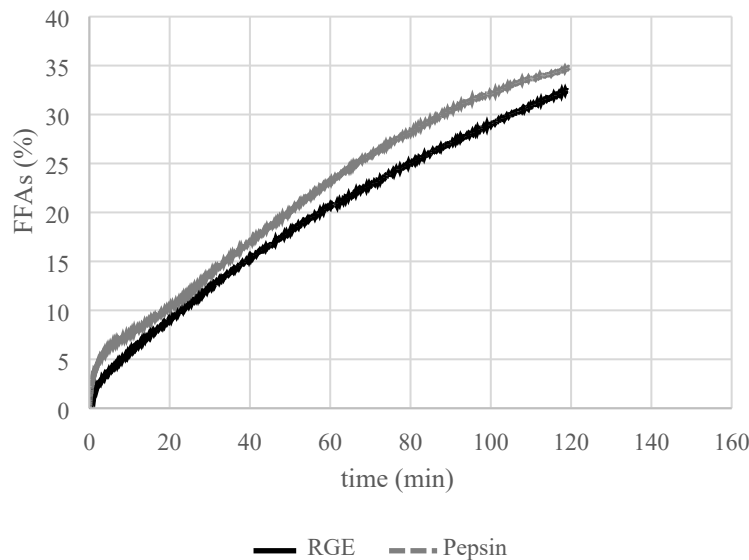


Fig. S6. Representative FFAs release kinetics (mass fraction of 0.25) during digestion from NaOH titration with pepsin or RGE addition in the gastric phase simulation.

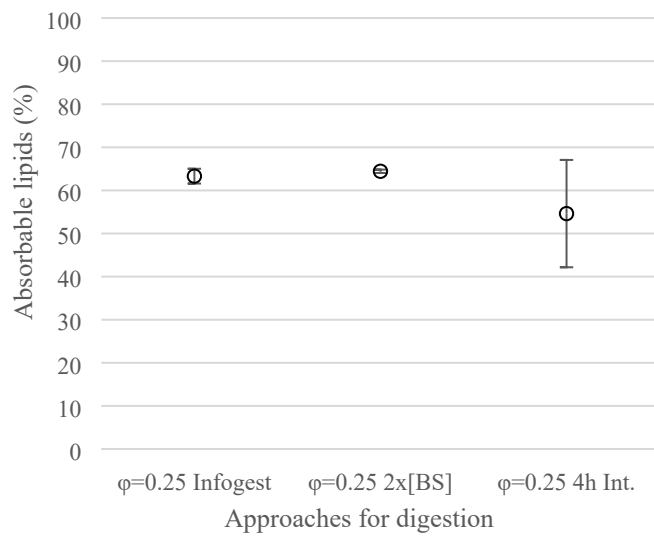


Fig. S7. Lipid bioaccessibility determined by quantifying the % of absorbable lipids in the micellar phase of the digesta at the end of the intestinal phase, comparing different approaches (INFOGEST protocol; same protocol with the doubling of the bile salt concentration (2x[BS]; same protocol with the doubling of the duration of the intestinal phase (4h Int)). This data set was obtained using emulsions with an initial oil mass fraction of  $\phi=0.25$ .

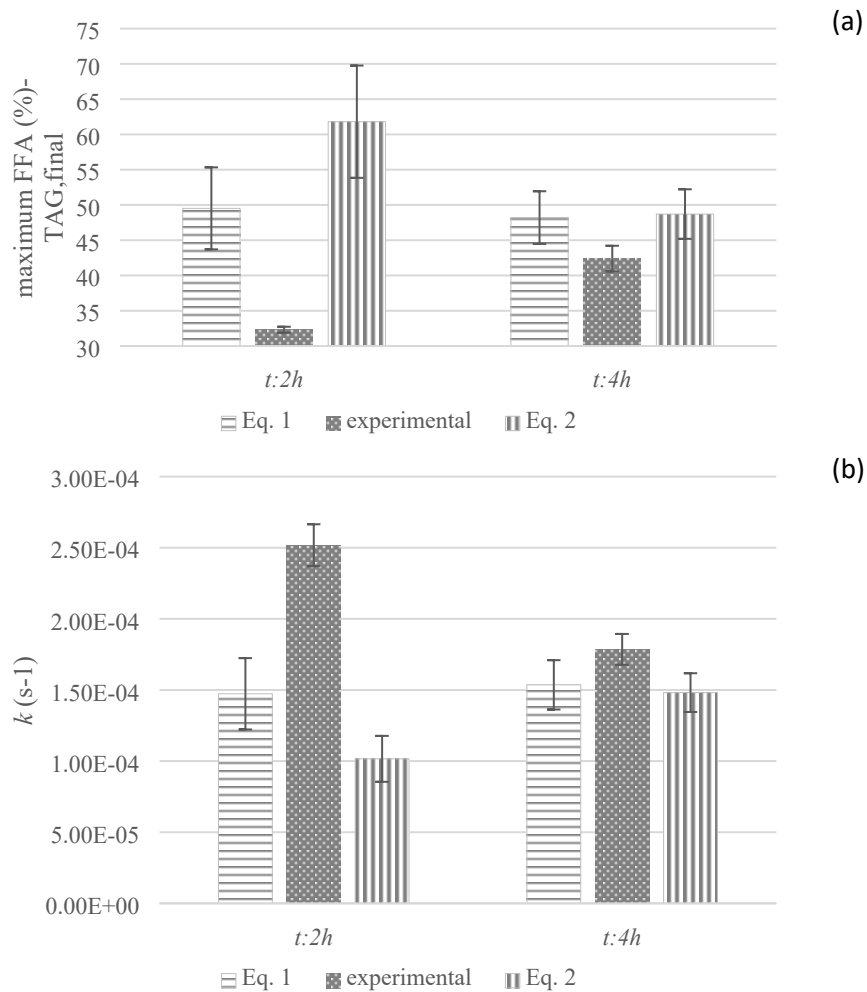


Fig. S8 Experimental and fitting parameters (Eqs. 1 and 2) for an initial lipid mass fraction of  $\phi=0.25$  comparing short ( $t: 2h$ ) and long ( $t: 4h$ ) *in vitro* intestinal digestion simulation. Maximum FFA released (a) and kinetic constant (b).